Electronic Supplementary Information (ESI)

Superior sodium storage performance of reduced graphene oxide-supported $Na_{3.12}Fe_{2.44}(P_2O_7)_2$/C nanocomposite

Hee Jo Song,[a,b] Kyeong-Ho Kim,[a] Jae-Chan Kim,[b] Seong-Hyeon Hong[a] and Dong-Wan Kim*[b]

[a] Department of Materials Science and Engineering, Seoul National University, Seoul 151-744, Republic of Korea

[b] School of Civil, Environmental and Architectural Engineering, Korea University, Seoul 136-713, Republic of Korea

Corresponding Author

* E-mail: dwkim1@korea.ac.kr (D.W. Kim)

Experimental procedures

Synthesis of NFP-NPs/C/rGO. All the chemicals used were reagent grade and employed without further purification. As mentioned above, NFP-NPs/C/rGO was synthesized by the sol-gel method; citric acid was used as the chelating agent as well as the carbon source. In a typical synthesis process, 8 g of a GO solution (2 wt% GO dispersion in water, Angstron Materials) was mixed with 42 ml of deionized water (total 50 ml). Next, 6.1 mmol of $Fe(CH_3COO)_2$ (Fe 29.5%, Alfa Aesar) and 15 mmol of citric acid (CA; 99.5%, Sigma-Aldrich) were dissolved in the aqueous GO dispersion. Then, 7.8 mmol of $Na(CH_3COO)$ (99%, Sigma-Aldrich) and 10 mmol of $NH_4H_2PO_4$ (98%, Sigma-Aldrich) were dissolved in another 50 ml of distilled water. The molar ratios of the Na/Fe/P/C sources were 3.12:2.44:4:6. The two solutions were then mixed in a three-neck round-bottom flask and refluxed at 80 °C for 12 h under magnetic stirring. After the reflux process, the solution was kept on a hotplate at 70 °C to evaporate the solvent. Next, the wet gel was completely dried in a vacuum oven. The resultant dried gel was then heat-treated in a tube furnace at 600 °C for 3 h in a flow of a 5% H_2/Ar balance gas. The product was ball-milled with ZrO_2 balls and ethanol, dried and then heat-treated again under the same conditions. For comparison, NFP-NPs/C without rGO was also synthesized under the same conditions.

Material characterization. Transmission electron microscopy (TEM) imaging was performed using a JEOL JEM-2100F system. Field-emission scanning electron microscopy (FESEM) imaging was performed using a Hitachi SU-70 system. The X-ray diffraction (XRD) patterns of the powder samples were measured with a Bruker D8-Advance system using Cu Kα radiation; the measurements were performed for 2θ of 10–40°. The Na, Fe, and P concentrations in solutions of the samples in HCl were determined using inductively coupled

plasma-optical emission spectroscopy (ICP-OES; ICP-730 ES, Varian). X-ray photoelectron spectroscopy (XPS) was performed with a Thermo Scientific Sigma Probe using an Al Kα X-ray source. The infrared (IR) spectra were measured in the range of 1400-400 cm^{-1} using an FT-IR spectrometer (Hyperion 3000, Bruker). The Brunauer–Emmett–Teller (BET) specific surface areas and pore size distributions of the products were determined based on their nitrogen adsorption–desorption isotherms, which were measured at 77 K using a Micromeritics ASAP 2010 system. The carbon contents of the powders were measured by thermogravimetric analysis (TGA; DTG-60H, Shimadzu Co.) and using an elemental analyzer (Flash EA 1112, Thermo Electron Co.).

Electrochemical measurements. The electrochemical properties of the NFP-NPs/C and NFP-NPs/C/rGO samples were evaluated using 2032 coin-type half cells, which were fabricated in an Ar-filled glove box. The NFP-NPs/C and NFP-NPs/C/rGO working electrodes were prepared using 70 wt% active material, 15 wt% Super P carbon black (MMM Carbon, Belgium), and 15 wt% polyvinylidene fluoride as binder (Sigma-Aldrich); this mixture was cast onto a piece of Al foil. The mass loading rate of the active material on the Al foil was 2~3 mg cm^{-2}. The cells were assembled using the working electrode, a glass microfiber separator film (diameter 47 nm, Whatman), and a piece of Na metal foil as the counter electrode. A liquid electrolyte consisting of 1 M $NaClO_4$ dissolved in a solution of ethylene carbonate and propylene carbonate in a volume ratio of 1:1 was used in the cells. These cells were galvanostatically cycled at voltages of 2.0–4.0 V (versus Na/Na^+) using an automatic battery cycler (WBCS3000, WonATech, Korea). Cyclic voltammetry (CV) measurements were performed for the same voltage range at a scan rate of 0.05 mV s^{-1}. Electrochemical impedance spectroscopy (EIS) measurements were performed in the frequency range of 100 kHz to 10 mHz at an AC amplitude of 10 mV; an Ivium-n-Stat (Ivium Technologies, Netherlands)

electrochemical test system was employed for the purpose.

Table S1. Na/Fe/P atomic ratios of NFP-NPs/C and NFP-NPs/C/rGO samples as determined by ICP-OES.

Sample	Element	No. of Moles	Atomic Ratio
NFP-NPs/C	Na	1.306	3.22
	Fe	0.984	2.43
	P	1.620	4.00
NFP-NPs/C/rGO	Na	1.338	3.29
	Fe	0.969	2.39
	P	1.624	4.00

Table S2. Results of C elemental analyses of NFP-NPs/C and NFP-NPs/C/rGO.

Sample	C content (wt%)
NFP-NPs/C	16.1
NFP-NPs/C/rGO	19.5

Table S3. Comparison of electrochemical performances of previously reported $Na_2FeP_2O_7$- and $Na_{3.12}Fe_{2.44}(P_2O_7)_2$-based cathodes for NIBs.

Material		**Voltage (V)**	**Cycle (No.)**	**Rate (C)**	**Capacity (mA h g^{-1})**	**Ref.**
$Na_2FeP_2O_7$	Submicron	2.0-4.0	10	0.05	82	[8]
$Na_2FeP_2O_7$	Micro	2.0-4.5	80	0.05	92	[20]
$Na_2FeP_2O_7$	Micro	2.0-3.8	50	0.05	80	[21]
$Na_2FeP_2O_7$	CNT composite	2.0-4.0	140	1	86	[22]
$Na_{3.12}Fe_{2.44}(P_2O_{7)2}$	Micro	1.7-4.0	60	0.05	80	[9]
$Na_{3.12}Fe_{2.44}(P_2O_{7)2}$	Graphene composite	1.7-4.0	80	0.2	100	[23]
$Na_{3.12}Fe_{2.44}(P_2O_{7)2}$	CNT composite	1.7-4.0	120	0.15	100	[24]
$Na_{3.12}Fe_{2.44}(P_2O_{7)2}$	Coral-like	2.0-4.0	200	5	80	[15]
$Na_{3.12}Fe_{2.44}(P_2O_{7)2}$	Hollow porous microspheres	1.5-4.0	500	10	60	[25]

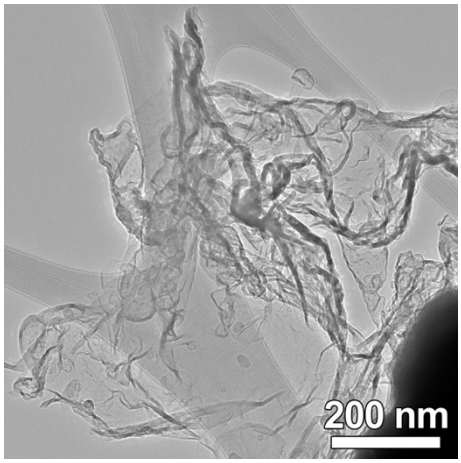

Fig. S1 TEM image of GO.

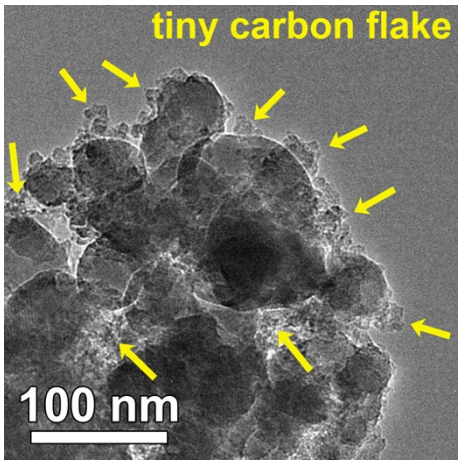

Fig. S2 TEM image of NFP-NPs/C (without rGO).

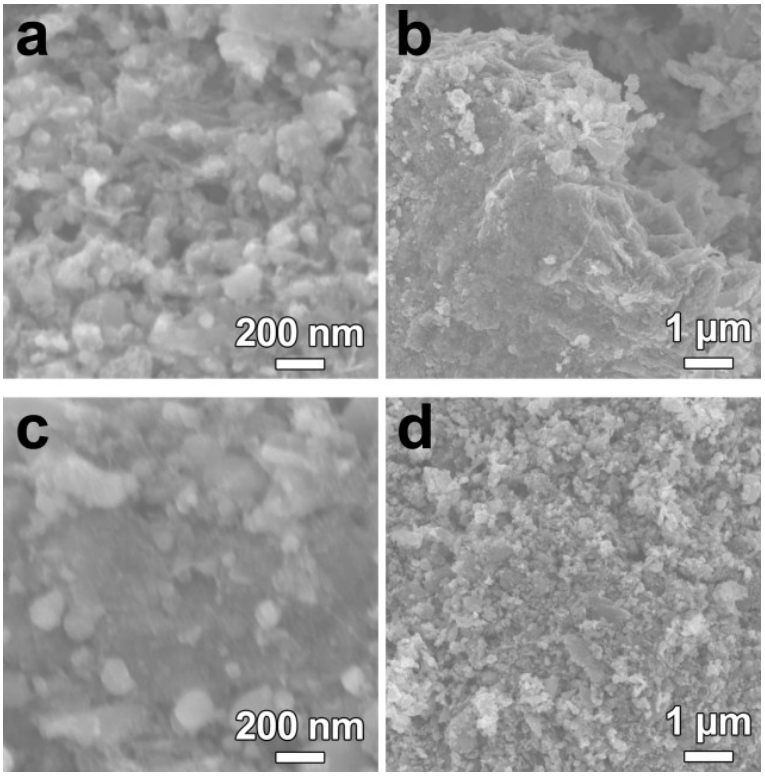

Fig. S3 FESEM images of (a-b) NFP-NPs/C/rGO after first HT process and (c-d) after HT→BM →HT process.

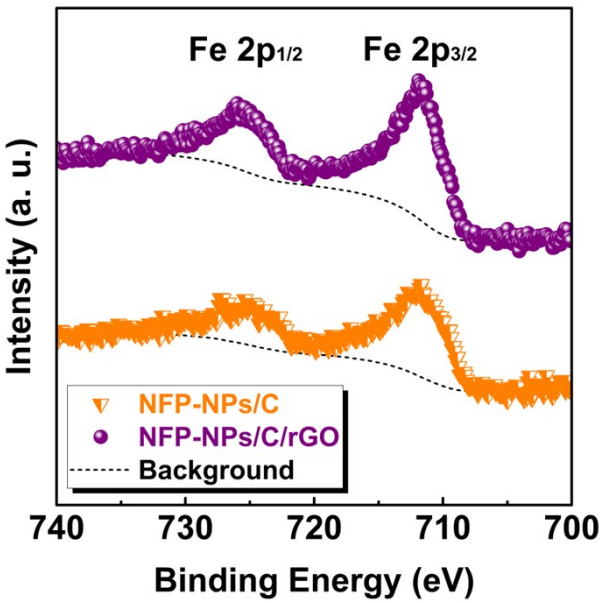

Fig. S4 Fe 2p levels XPS spectra of NFP-NPs/C and NFP-NPs/C/rGO.

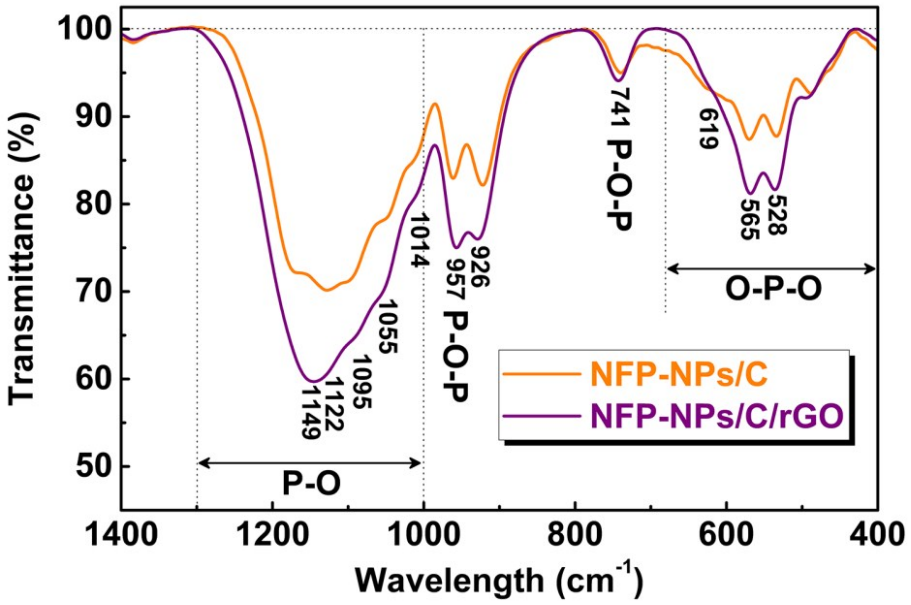

Fig. S5 FT-IR spectra of NFP-NPs/C and NFP-NPs/C/rGO in the range of 1400-400 wavelength (cm^{-1}).

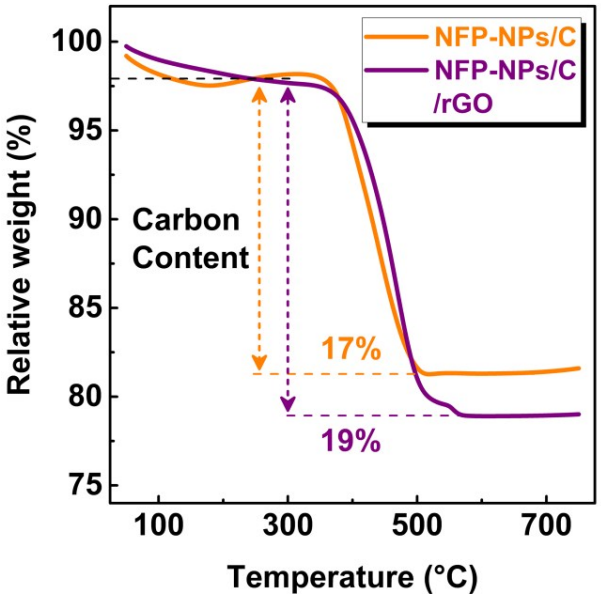

Fig. S6 TGA curves of NFP-NPs/C and NFP-NPs/C/rGO.

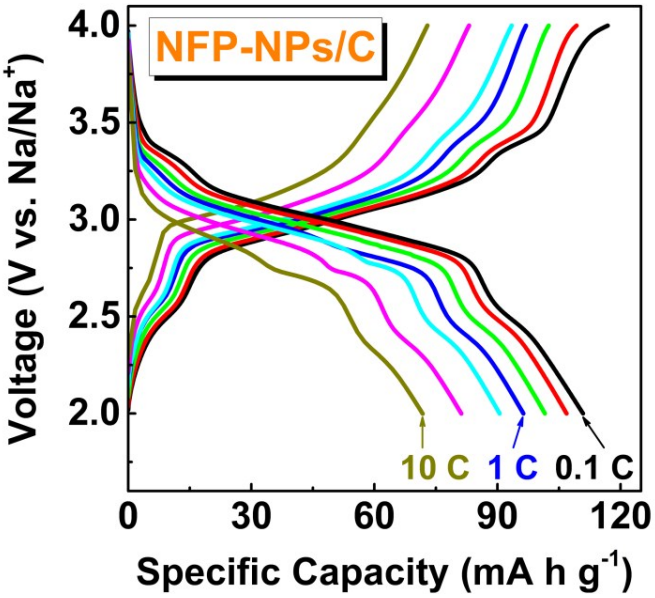

Fig. S7 Galvanostatic voltage–capacity profiles of NFP-NPs/C at different rates.

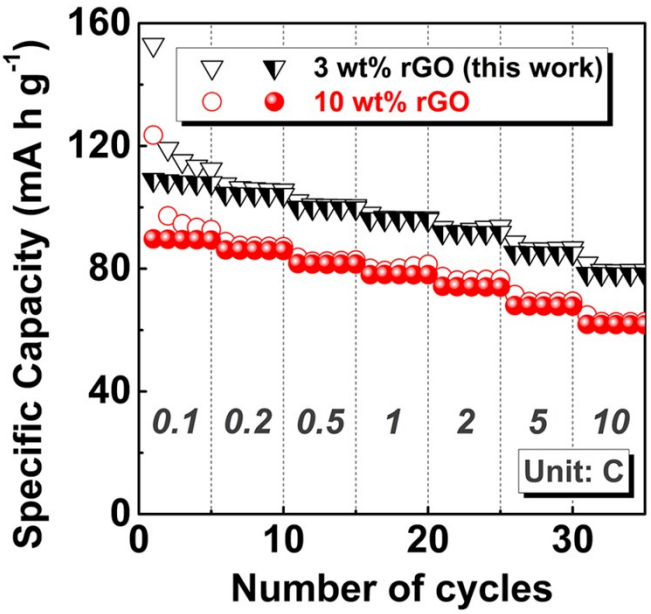

Fig. S8 Rate performance of NFP-NPs/C/rGO with different amount of rGO in nanocomposite.

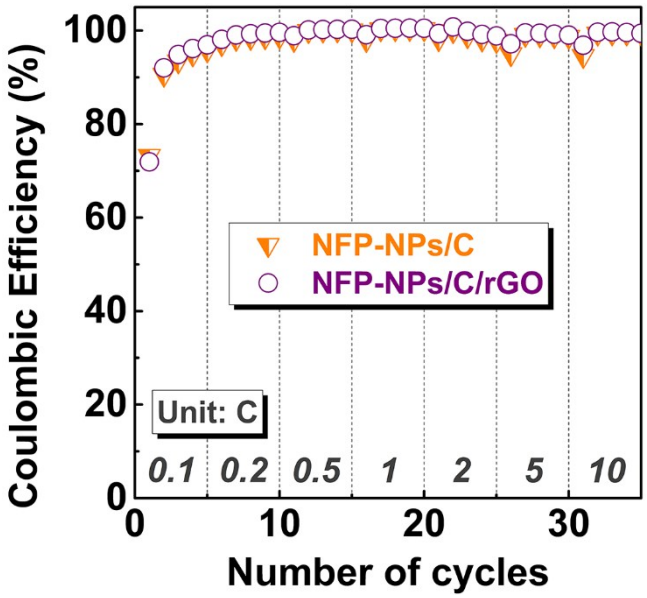

Fig. S9 Coulombic efficiency of NFP-NPs/C and NPF/NPs/C/rGO.

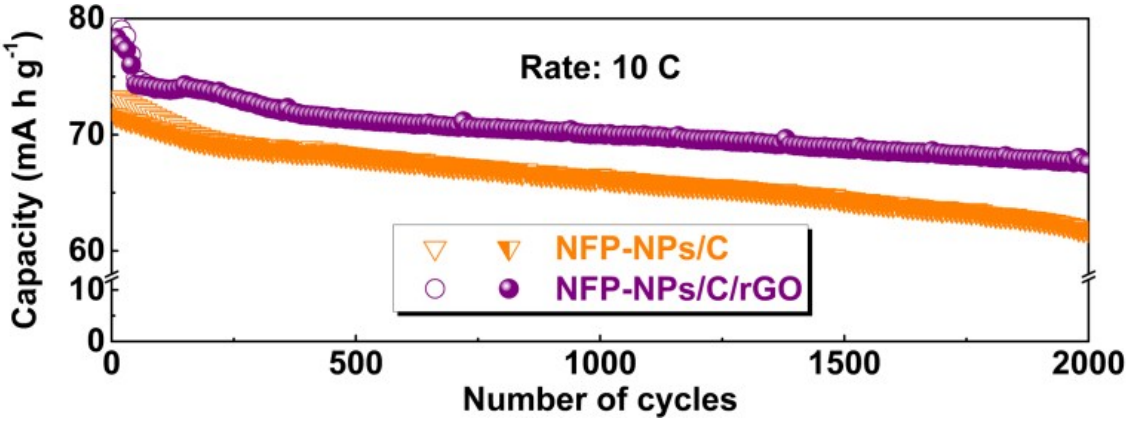

Fig. S10 Long-term cyclability of NFP-NPs/C and NFP-NPs/C/rGO at 10 C.